

Comparison of reactive species generation in different cold plasma sources

J. Van der Paal, Y. Gorbanev, E. Helsen, W. Van Boxem, E. Biscop and A. Bogaerts
Research Group PLASMANT, Department of Chemistry, University of Antwerp, Belgium

Abstract: A number of chemical kinetics models are developed to assess the ability of the COST-jet, kINPenIND, SOFT-jet and FE-DBD device to generate various reactive oxygen and nitrogen species (RONS) when treating a liquid surface. Different approaches are proposed to model the interplay between gas and liquid phase chemistry in (i) the plasma jet devices and (ii) the DBD set-up. The results of our models are validated by colorimetric measurements of H_2O_2 and NO_2^- for various conditions.

Keywords: Chemical kinetics models, RONS, Plasma Sources, Plasma jet, DBD

1. Introduction

In the last decades, cold atmospheric plasmas (CAPs) have been investigated for numerous medical applications, ranging from decontamination of wounds and accelerating wound healing [1], to the use as cancer treatment modality [2], with highly promising results obtained in all these domains. However, throughout the years, many different plasma sources have been developed by numerous researchers. Indeed, although for medical applications, mainly dielectric barrier discharge (DBD) and plasma jet designs have been used, there exist many variations in (i) dimensions of these devices, (ii) electrode configuration, (iii) operation frequency, (iv) feed gas composition, and many other parameters. As all these differences alter the plasma chemistry and physics, it is extremely difficult to compare treatment outcomes.

Despite the use of all these different plasma source set-ups, the plasma-generated reactive oxygen and nitrogen species (RONS) play a predominant role in the mediation of medical effects (e.g., the sterilization of tissue, the acceleration of wound healing or the killing of cancer cells). These species are generated due to the presence of molecular oxygen and nitrogen in the feed gas (either as impurities or as additives), or due to interaction of the plasma with ambient air. Once they reach the surface being treated, they will interact with biological substrates, thereby triggering a response in the treated sample.

In the present study, chemical kinetics simulations are combined with colorimetric measurements to assess the ability of different plasma sources to generate RONS. More specifically, three plasma jet sources (kINPen IND, COST-jet and SOFT-jet) and a FE-DBD device are investigated. Knowledge of which species are dominant in each of these devices will, in the future, allow researchers to link biological outcomes with specific species. In the experimental liquid measurements, we focus on H_2O_2 and NO_2^- , which are two of the most important long-lived species. Combining these measurements with the chemical kinetics model allows us to investigate the pathways leading to these species, and to discuss in detail the different plasma chemistry in all sources.

2. Methods

2.1. Plasma sources

The so-called COST-jet was developed as a reference jet, and has been described in detail in literature. [3] The kINPen IND is a commercial plasma source and has also been reviewed extensively in literature. [4] The SOFT-jet was developed at PBRC. In comparison to the COST-jet and the kINPen, which use helium or argon as a carrier feed gas, respectively, this plasma jet uses a discharge in ambient air. [5] Lastly, the floating electrode dielectric barrier discharge (FE-DBD) device, developed at Drexel University, is added to the comparison. It has already been used in various *in vitro/in vivo* cancer treatment studies, in which the set-up of the source is described in detail as well. [6] The different conditions used in this study are summarized in Table 1.

Table 1: Operating conditions of the different plasma sources used in this study.

Plasma source	Variations in conditions
COST-jet (Helium)	Addition of H_2O to the feed gas (0-20 % relative saturation) Flow rate = 1 slm Treatment distance = 10 mm Treatment time = 180 s
kINPen IND (Argon)	Treatment distance = 10-30 mm Treatment time = 300-420 s Flow rate = 3 slm
SOFT-jet (Air)	Treatment distance = 2-3 mm Treatment time = 300-1200 s Flow rate = 1 slm
DBD (Air)	Treatment distance = 1 mm Treatment time = 10 s Operating frequency = 250-500 Hz

2.2. Liquid measurement

After treatment of 2 mL PBS in 12-well plates (kINPen IND, SOFT-jet and DBD device) or 0.2 mL PBS in a 96-well plate (COST-jet), the measurements of H_2O_2 were done using the colorimetric method with the Ti(IV) reagent, as described in previous works. [7] The NO_2^- -concentration after plasma treatment was performed using colorimetry in a reaction with Griess reagent, provided as

the Griess Reagent Nitrite Measurement kit. The details of these measurements are also described elsewhere. [7]

2.3. Chemical kinetics models

Chemical kinetics models are used to investigate the chemistry occurring in the different sources mentioned above. Both the gas phase and liquid phase are included in the models. The input parameters (e.g., power input, gas flow rate, plasma source dimensions or operating gas temperature) of the kinetic models are modified to allow developing specific models for each plasma source, including all different conditions used experimentally.

To describe the three plasma jet sources, in each case, two separate models are used to simulate the chemistry occurring in (i) the gas phase and (ii) the liquid phase separately. This approach is based on a model developed by Lietz *et al.* [8], and has been used before to describe the chemistry occurring in the gas and liquid phase of the kINPen IND. [9] The gas phase simulation follows an infinitesimal volume element along the plasma axis, starting inside the jet and ending when the plasma reaches the liquid surface. The displacement of this volume element is coupled with the simulation time (main variable in a chemical kinetics model) by the gas velocity. As the gas velocity decreases in the effluent of the plasma jets, there is a non-linear relation between time and distance, as is illustrated by comparing top and bottom x-axis in Figure 1. The final densities of 32 species (most important species out of a total of 94 gas phase species) are then used as an input for the liquid phase simulation, in which the transport of the species to the liquid phase is based on Henry's law.

To describe the DBD device, on the other hand, both gas phase and liquid phase are coupled in one model. This different approach is used, as in this case, the entire volume between the electrode and the liquid is considered as a homogenous plasma in which the power is dissipated. Therefore, the entire plasma volume is always in contact with the liquid surface. During each time step, three processes occur in the model:

- i. Gas phase chemistry, based on the gas phase reactions included in the chemistry set.
- ii. Diffusion of gas phase species into the liquid (or evaporation of liquid species if oversaturation occurs), based on the density of each species in the gas and liquid phase, their Henry constant and gas phase diffusion constant.
- iii. Liquid phase chemistry, based on the liquid phase reactions included in the chemistry set.

3. Reactive species generation

3.1 COST-jet

Figure 1 shows the chemical kinetics modeling results in the gas phase of the COST-jet, in the case of 5% H₂O added to the helium feed gas. This illustrates that HNO₂ is entirely generated in the device (region illustrated by the

grey color), due to N₂ and O₂ impurities present in the feed gas. In the case of H₂O₂ on the other hand, a large fraction of the final concentration is generated in the effluent of the COST-jet, which is mainly due to recombination of OH radicals generated inside the active plasma region. The N₂ density is also shown in Figure 1, as an illustration of the mixing with ambient air, which is implemented in the effluent of all plasma jets. Inside the COST-jet, the N₂ density is due to impurities present in the feed gas. However, in the effluent, its concentration rises drastically, due to inflow of ambient air species (in our model, we take N₂, O₂ and H₂O into account as ambient air species). The rate of this mixing is based on 2D fluid dynamics simulations.

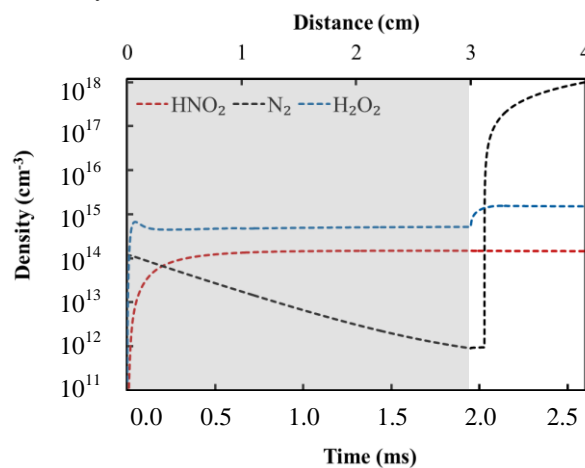


Fig. 1. Illustration of the gas phase calculation results of the COST-jet, in the case of 5% H₂O addition to the feed gas. The grey zone illustrates the region inside the COST-jet (3 cm), whereas the white zone is the effluent of the jet (1 cm).

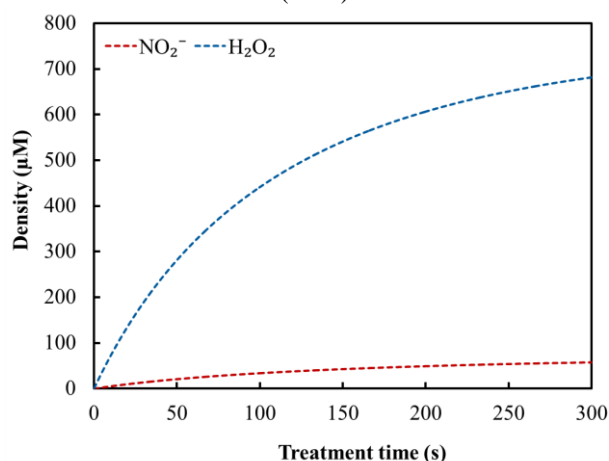


Fig. 2. Illustration of the calculation results for the generation of H₂O₂ and NO₂⁻ in the liquid phase, after contact of the effluent of the COST-jet with a liquid surface.

The final densities of these gas phase simulations, i.e., obtained at the liquid surface (4 cm in Figure 1) are then

taken as an input for the liquid phase simulation, of which an example of calculation results is shown in Figure 2.

3.2 DBD device

Figure 3 shows the results of the chemical kinetics model in the gas phase of the DBD device, at an operating frequency of 250 Hz. This illustrates that HNO_2 and H_2O_2 are mostly generated during the pulses (or filaments), but are stable enough to maintain a high density in the interpulse region. Short-lived species, such as OH radicals ($\bullet\text{OH}$), on the other hand, are lost during in the interpulse region, *i.e.*, when no power is applied. These results also indicate that the densities of all species inside the plasma region evolve towards equilibrium. At that point, generation from recombination of short-lived species and loss due to reactions with these same species are in chemical equilibrium.

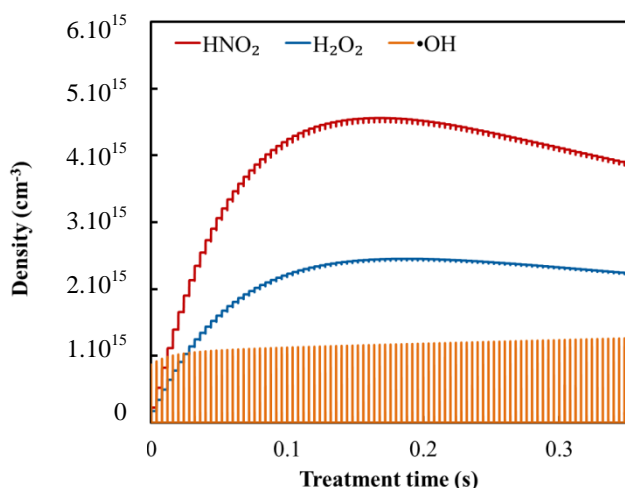


Fig. 3. Illustration of the calculation results for the generation of H_2O_2 , NO_2^- and $\bullet\text{OH}$ in the gas phase of the DBD device, at an operating frequency of 250 Hz.

In the 0D approach of DBD-treatment of a liquid surface, these gas phase species are always in contact with the liquid surface, which is included in the model by applying Henry's law at each time step. The calculation results for H_2O_2 and NO_2^- in the liquid phase are shown in Figure 4, which indicates a steady increase of both long-lived species with increasing treatment time.

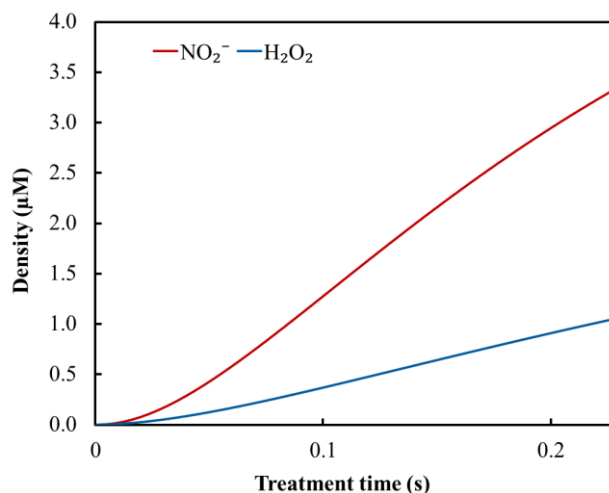


Fig. 4. Illustration of the calculation results for the accumulation of H_2O_2 and NO_2^- in the DBD-treated liquid. Because of the coupling between gas and liquid phase, and the short time-steps needed to capture the pulses, the calculations are very time-consuming, so results could only be obtained at this stage for 0.2 s.

3.3 Discussion

The results of the other treatment conditions and plasma sources look very similar as the ones presented in Figures 1 - 4. We use the colorimetric measurement results to validate our models. Currently the agreement is not yet good enough, so we need to further improve our models. We are working on several improvements, including:

- i. Adding photo-ionization and photolysis reactions to the chemistry set of our models. We expect these to be particular important in the case of the DBD device and for the plasma jets when the discharge is in contact with the liquid surface.
- ii. Effect of turbulence in the liquid on the Henry's constants, in the case of the plasma jet devices with a strong axial flow rate.

Once the models are validated, we can use the results of the underlying chemistry to discuss the generation of the species investigated (H_2O_2 and NO_2^-), as well as all other biological relevant species included in the models, in detail.

4. Conclusion

In this research, we have shown the first results of different chemical kinetics models for multiple plasma sources. The goal of this research is to develop robust models, which allow predicting the species generated by different plasma sources used in biological applications of cold plasmas, as well as studying the underlying chemistry. Knowing the density of all species generated might allow us in the future to couple biological outcomes to certain important species, and can help tuning the

operating conditions to optimize the treatment to be as effective as possible.

5. Acknowledgements

We acknowledge financial support from the Fund for Scientific Research (FWO) Flanders via Grant No. 11U5416N. The computational resources and services used in this work were provided by the VSC (Flemish Supercomputer Center), funded by the Research Foundation - Flanders (FWO) and the Flemish Government – department EWI.

6. References

- [1] G. Lloyd, G. Friedman, S. Jafri, G. Schultz, A. Fridman, and K. Harding, “Gas plasma: Medical uses and developments in wound care,” *Plasma Process. Polym.* **7**, 194–211 (2010).
- [2] M. Keidar, “Plasma for cancer treatment,” *Plasma Sources Sci. Technol.* **24**, 033001 (IOP Publishing, 2015).
- [3] J. Golda, J. Held, B. Redeker, M. Konkowski, P. Beijer, A. Sobota, G. Kroesen, N. St. J. Braithwaite, et al., “Concepts and characteristics of the ‘COST Reference Microplasma Jet,’” *J. Phys. D Appl. Phys.* **49**, 84003–84011 (IOP Publishing, 2016).
- [4] S. Reuter, T. von Woedtke, and K. Weltmann, “The kINPen—a review on physics and chemistry of the atmospheric pressure plasma jet and its applications,” *J. Phys. D. Appl. Phys.* **51**, 233001 (IOP Publishing, 2018).
- [5] P. Attri, J. Gaur, S. Choi, M. Kim, R. Bhatia, N. Kumar, J.-H. Park, A. E. Cho, E. H. Choi, et al., “Interaction studies of carbon nanomaterials and plasma activated carbon nanomaterials solution with telomere binding protein,” *Sci. Rep.* **7**, 2636 (Springer US, 2017).
- [6] A. Lin, Y. Gorbanev, J. De Backer, J. Van Loenhout, W. Van Boxem, F. Lemi re, P. Cos, S. Dewilde, E. Smits, et al., “Non-Thermal Plasma as a Unique Delivery System of Short-Lived Reactive Oxygen and Nitrogen Species for Immunogenic Cell Death in Melanoma Cells,” *Adv. Sci.* **6**, 1802062 (2019).
- [7] Y. Gorbanev, J. Van Der Paal, W. Van Boxem, S. Dewilde, and A. Bogaerts, “Reaction of chloride anion with atomic oxygen in aqueous solutions : Can cold plasma help in chemistry research?,” *Phys. Chem. Chem. Phys.* **21**, 4117–4121 (2019).
- [8] A. M. Lietz and M. J. Kushner, “Air plasma treatment of liquid covered tissue : long timescale chemistry,” *J. Phys. D. Appl. Phys.* **49**, 425204 (IOP Publishing, 2016).
- [9] W. Van Boxem, J. Van der Paal, Y. Gorbanev, S. Vanuytsel, and E. Smits, “Anti-cancer capacity of plasma- treated PBS : effect of chemical composition on cancer cell cytotoxicity,” *Sci. Rep.* **7**, 16478 (Springer US, 2017).